On the Uncertainty Analysis of Shape Reconstruction from Areas of Silhouettes

Amyn Poonawala
University of California, Santa Cruz
amyn@ce.ucsc.edu

Peyman Milanfar
University of California, Santa Cruz
milanfar@ee.ucsc.edu

Richard Gardner
Western Washington University, Bellingham
Richard.Gardner@wwu.edu

Abstract

We address the inverse problem of shape reconstruction of a convex object from noisy measurements of the areas of its silhouettes (shadows) in several directions. Such data represent values of the brightness function of the object, which in the 2-D case is simply a phase-shifted version of its diameter (width) function. In the past, we have proposed non-linear and linear algorithms for reconstructing an n-dimensional convex body using finitely many noisy measurements of its brightness function. Here we carry out a statistical uncertainty analysis of the problem for the 2-D case by generating asymptotic confidence regions around the underlying shape. Confidence regions conveniently display the effect of experimental parameters like eccentricity, scale, noise power, viewing direction set, on the quality of the estimated shape. We also present a statistical performance analysis of our proposed linear algorithm using global confidence regions.

1. Introduction

The "shape from silhouettes" technique has been extensively used in computer vision to reconstruct 3-D objects using multiple 2-D shadows; see [1] and [8]. However we consider a much weaker form of data where each measurement provides only the area of the silhouette and absolutely no information about its shape or location. In general the problem we consider is that of reconstructing an n-dimensional object using measurements of its brightness function, that is, the function giving the $(n-1)$-dimensional volume of its orthogonal projections (i.e., silhouettes) on hyperplanes. The problem is important in geometric tomography, the area of mathematics concerning the retrieval of information about a geometric object from data about its sections or projections (see [2]).

Consider an imaging scenario using a single pixel CCD camera (for example, a photodiode element) or an object in the far field of a camera which is so severely ill-resolved that its entire image falls on a single pixel at any given time (e.g., the lightcurves obtained in asteroid imaging as in [5]). In such cases the intensity of the pixel is proportional to a brightness function value of the object. For the 2-D case, an application arises in robotics when the diameter (width) of a shape is measured using a parallel-jaw gripper as in [13]. Brightness functions can also be used for target reconstruction using Doppler-resolved laser radar data (see [9]).

In this paper, we study the uncertainty associated with estimating a shape from its noisy brightness function values. We formally introduce the problem and the Extended Gaussian Image (EGI) parameterization in Section 2. Section 3 presents a novel statistically efficient way to obtain cartesian coordinates of a 2-D shape from its corrupted EGI values. In Section 4 we develop confidence regions around the underlying shape using the technique described by Ye, et al in [14].

The maximum likelihood estimator (MLE), a statistically optimal algorithm, involves constrained non-linear optimization and thus has little practical use. Therefore in [4] and [11], we proposed a linear estimation algorithm, "Algorithm BrightLSQ," for reconstructing a shape using noisy brightness function values. However we incur a performance loss by employing this algorithm (instead of the MLE) and in Section 5 we use confidence regions in a statistical performance analysis of the linear algorithm. This will enable us to assess the quality of the shape estimates obtained from the linear algorithm and to compare its performance to that of the optimal one.

2. Shape from area of silhouettes

The brightness function $b(\mathbf{v})$ of a suitably smooth convex body for a given viewing direction $\mathbf{v}$ (a unit vector) is given by

$$b(\mathbf{v}) = \frac{1}{2}\int_S |\mathbf{u}^T\mathbf{v}| f(\mathbf{u})\, d\mathbf{u}, \qquad (1)$$

where $f(\mathbf{u})$ is the extended Gaussian image (EGI) of the body. Integration is over the unit sphere S (in two dimensions, the unit circle). The quantity $f(\mathbf{u})$ is actually just the reciprocal of the curvature at the point on the boundary where $\mathbf{u}$ is the outer unit normal vector. (For more details, see [3], [4], and [6].) A convex body is determined uniquely, up to translation, by its EGI. For an N-sided polygon, the EGI can be simply represented by the N vectors

$a_k\mathbf{u}_k$, each along the outer normal $\mathbf{u}_k$ to an edge of the polygon and with magnitude equal to the length a_k of that edge. If $\mathbf{u}_k = [\cos\theta_k, \sin\theta_k]^T$ and $\mathbf{v} = [\cos\alpha, \sin\alpha]^T$, the brightness function of this polygon, by (1), is

$$b(\alpha) = \frac{1}{2}\sum_{k=1}^{N} a_k |\cos(\alpha - \theta_k)|. \tag{2}$$

The brightness function in the 2-D case simply equals the length of the shadow and the only missing information, provided by the silhouette, is the position of the shadow. Nevertheless, this is enough to cause substantial non-uniqueness problems. Whereas a planar convex body is uniquely determined by all its silhouettes, there can be infinitely many convex bodies with the same (exact) brightness function measurements from all viewing directions. However, Aleksandrov's projection theorem [2, Theorem 3.3.6] says that any two origin-symmetric convex bodies with the same brightness functions must be equal. (An *origin-symmetric* body is one equal to its reflection in the origin.) By seeking only to reconstruct origin-symmetric convex bodies, we therefore avoid this non-uniqueness issue.

The problem is to estimate the shape using corrupted brightness function values measured from multiple viewing directions. The noise throughout the discussion is assumed to be Gaussian white noise with variance σ^2 and the problem is solved in two steps. In Step 1, the shape parameters $a_1, \ldots, a_N$ and $\theta_1, \ldots, \theta_N$ (i.e., the EGI of an approximating polygon) are estimated from the noisy brightness function values, and in Step 2 these estimated parameters are used to obtain a more direct cartesian coordinate representation of the shape. We have proposed non-linear and linear algorithms for Step 1 in [3] and [4]; the next section presents a systematic analysis of Step 2 from the estimation perspective.

3. Shape from EGI

The simplest way to obtain shape from EGI is to arrange the vectors in counterclockwise order, rotate each vector counterclockwise by $\pi/2$, and place them so that the tail of each vector lies at the head of the preceding vector (see Fig. 1 and [10]). Then, if the EGI is $\{a_1, \ldots, a_N, \theta_1, \ldots, \theta_N\}$, the vertices of the reconstructed polygon are

$$z_t = \sum_{k=1}^{t} a_k e^{i(\theta_k + \pi/2)}, \tag{3}$$

where $z_t = x_t + iy_t$ is the complex number representing the vertex $\mathbf{z}_t = (x_t, y_t)$, $t = 1, \ldots, N$.

Unfortunately this simple approach is not suitable for our statistical analysis. The reason is that since the EGI is estimated using noisy measurements of the brightness function, it too will be corrupted. In this case (3) is inappropriate, because it does not determine the vertices independently; rather, the position of each vertex depends on that of the preceding vertices. This causes the error in vertex position to accumulate as the vertex index t increases from $t = 1$ to $N/2$. (After $t = N/2$ it decreases due to the symmetry assumption; for more details see [11] and [12]). The main goal of this section is to overcome this problem.

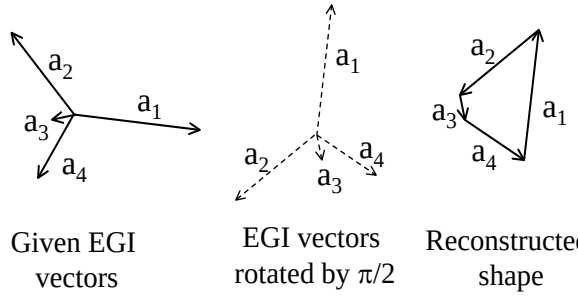

Figure 1: Cartesian shape representation from EGI.

Thus our basic aim is estimate $\mathbf{z} = [z_1, \ldots, z_N]^T$ so that the error is evenly distributed among its components. From (3) we have

$$z_t - z_{t-1} = a_t e^{i(\theta_t + \pi/2)}, \tag{4}$$

for $t = 1, \ldots, N$, and hence the equation

$$\mathbf{Q}\mathbf{z} = \mathbf{r}, \tag{5}$$

where

$$\mathbf{Q} = \begin{bmatrix} -1 & 1 & 0 & \cdots & 0 & 0 \\ \vdots & \vdots & \vdots & & \vdots & \vdots \\ 0 & 0 & 0 & \cdots & -1 & 1 \\ 1 & 0 & 0 & \cdots & 0 & -1 \end{bmatrix}$$

and

$$\mathbf{r} = \left[a_1 e^{i(\theta_1 + \pi/2)}, \ldots, a_N e^{i(\theta_N + \pi/2)}\right]^T.$$

However, rank $\mathbf{Q} = N - 1$, so the solution for $\mathbf{z}$ in (5) is not unique. To deal with this, we observe that we may fix the centroid of the polygon at the point with complex number form c by adding the constraint

$$\frac{1}{N}\sum_{t=1}^{N} z_t = c. \tag{6}$$

When c is the origin, this can be written in the form $\mathbf{e}^T\mathbf{z} = 0$, where $\mathbf{e} = [1, 1, \ldots, 1]^T$. Appending this constraint to (5) we obtain

$$\tilde{\mathbf{Q}}\mathbf{z} = \tilde{\mathbf{r}}, \tag{7}$$

where $\tilde{\mathbf{Q}} = [Q, \mathbf{e}]^T$ is $(N+1) \times N$ with full rank N and $\tilde{\mathbf{r}} = [\mathbf{r}, 0]^T$ is $(N+1) \times 1$. Therefore we can solve (7)

uniquely using linear least squares optimization by $\mathbf{z} = \mathbf{D}\tilde{\mathbf{r}}$, where

$$\mathbf{D} = (\tilde{\mathbf{Q}}^T\tilde{\mathbf{Q}})^{-1}\tilde{\mathbf{Q}}^T = [\mathbf{d}_1, \mathbf{d}_2, \ldots, \mathbf{d}_N]^T, \quad (8)$$

say, with $\mathbf{d}_t^T = [d_{t1}, \ldots, d_{t(N+1)}]^T$ for $t = 1, \ldots, N$. Since the last component of $\tilde{\mathbf{r}}$ is zero, this gives

$$z_t = \mathbf{d}_t^T\tilde{\mathbf{r}} = \sum_{k=1}^{N} d_{tk}a_k e^{i(\theta_k+\pi/2)}. \quad (9)$$

Comparing (9) with (3), we see that z_t now depends on all the EGI vectors. We can show (see [11]) that this method distributes error more evenly.

4. Confidence Region Analysis

Asymptotic confidence regions are used to analyze and visualize the performance of 2-D parametric shape estimators. Assuming a maximum likelihood estimator (MLE) operating in the asymptotic regime, the Cramér-Rao lower bound (CRLB) for the shape parameters can be used to define a confidence region around the true boundary of the shape. In our analysis below, we follow [14]. Note that the MLE is asymptotically normal, unbiased, and asymptotically attains the CRLB; see [7, pp. 164–167].

Consider a 2-D shape parameterization $\mathbf{s}(t;\mathbf{\Psi})$, giving the cartesian coordinates of the point on the boundary of the object at the point indexed by $t \in [0, T]$. Here $\mathbf{\Psi} \in \Re^P$ is the P-dimensional parameter vector. At each point along the boundary (i.e., for all $t \in [0, T]$) we determine a local confidence region $U_\beta(t) \subset \Re^2$ centered at the true point $\mathbf{s}(t;\mathbf{\Psi})$. The size of the local confidence region depends on the chosen local confidence level $\eta \in [0, 1]$; β is calculated such that $\Pr\{X \leq \beta^2 = \eta\}$, where X is chi-square with two degrees of freedom. Then, if $\hat{\mathbf{s}}_{MLE}(t)$ is estimated using an MLE operating in the asymptotic regime, we have

$$\Pr\{\hat{\mathbf{s}}_{MLE}(t) \in U_\beta(t)\} = \eta. \quad (10)$$

The local confidence region $U_\beta(t)$ for $\mathbf{s}(t)$ is given by

$$U_\beta(t) = \{\mathbf{x} \in \Re^2 : (\mathbf{x} - \mathbf{s}(t))^T\mathbf{C}_\mathbf{s}(t)^{-1}(\mathbf{x} - \mathbf{s}(t)) \leq \beta^2\}, \quad (11)$$

where

$$\mathbf{C}_\mathbf{s}(t) = \nabla_\mathbf{\Psi}\mathbf{s}(t;\mathbf{\Psi})\mathbf{C}_\mathbf{\Psi}\left[\nabla_\mathbf{\Psi}\mathbf{s}(t;\mathbf{\Psi})\right]^T \quad (12)$$

is the 2×2 covariance matrix of $\mathbf{s}(t;\mathbf{\Psi})$ depending on the CRLB $\mathbf{C}_\mathbf{\Psi}$ for the estimated parameters. A global confidence region can now be obtained by moving $U_\beta(t)$ along the boundary:

$$U_\beta = \bigcup_{t\in[0,T]} U_\beta(t). \quad (13)$$

The asymptotic global confidence region defines an uncertainty band around the entire boundary of the true shape.

For an N-sided polygon we have $\mathbf{\Psi} \in \Re^{2N}$. Then $\mathbf{s}(t)$ is defined using (9) and $\mathbf{C}_\mathbf{\Psi}$ is calculated following the procedure outlined in [12]. The local confidence region for each vertex ($t = 1, \ldots, N$) is an ellipse, calculated using (11) and (12).

Fig. 2 shows the local confidence ellipses for an origin-symmetric, regular polygon with $N = 12$ sides. The brightness function was measured from 36 equally spaced viewing angles in the range $[0, \pi]$, with noise strength $\sigma = 0.1$ and local confidence level $\eta = 0.73$ for all the ellipses. Note that the local confidence regions for all the vertices are of the same size since the underlying polygon is equilateral and equiangular. (This is not true if (3) is used instead of (9); see [11]. This is due to the error accumulation effect mentioned in Section 3.) The global confidence regions can be similarly obtained from (13) by allowing the parameter t to take continuous values in the range $[0, N]$; see [11].

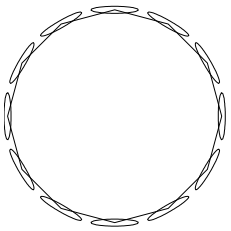

Figure 2: Confidence regions for a regular polygon.

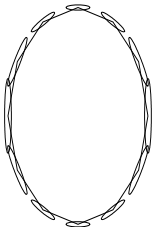

Figure 3: Confidence regions for an affinely regular polygon.

Fig. 3 shows the local confidence regions for an affinely regular polygon with the same experimental parameters as above. The polygon is stretched along the vertical direction and therefore a uniform viewing set provides more information along the horizontal direction thereby resulting in unequally sized ellipses.

5. Experimental Results and Performance Analysis

Fig. 4 illustrates true (solid line) and estimated (dotted line) polygons obtained using our linear algorithm (specifically, Algorithm BrightLSQ from [4] with a post-processing step called decimation, described in [11], that reduces to a prescribed number N the edges of the output polygon). The experiment was performed using the same underlying polygon, noise power and viewing set as used in Fig. 2. The local and global confidence regions corresponding to a local confidence level $\eta = 0.8$ are also shown for better illustration.

A performance analysis of an algorithm can be carried out by comparing it with the optimal algorithm via the local and global confidence regions. Note that the MLE operating in the asymptotic regime is in fact the statistically optimal algorithm since it is asymptotically unbiased and attains the CRLB. Recall that the confidence regions developed in Section 4 are for the MLE operating in asymptotic regime. In this section, we analyze the performance of our proposed linear algorithm using global confidence regions (for a performance analysis using local confidence regions see [11]).

Let $\hat{\mathbf{s}}$ be the estimated shape boundary resulting from a given algorithm and define the corresponding error probability e by

$$e = 1 - \Pr\{\hat{\mathbf{s}} \in U_\beta\} \tag{14}$$

Thus e is the probability that the estimated boundary $\hat{\mathbf{s}}$ does not lie completely inside the global confidence region U_β. Let $\hat{\mathbf{s}}_{MLE}$ and $\hat{\mathbf{s}}_{alg}$ be the estimated shape boundary obtained using the MLE and the linear algorithm respectively.

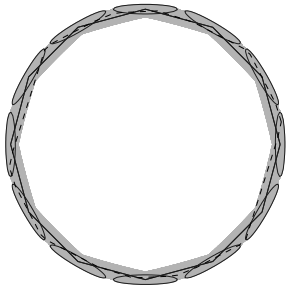

Figure 4: True and estimated polygons with global confidence region.

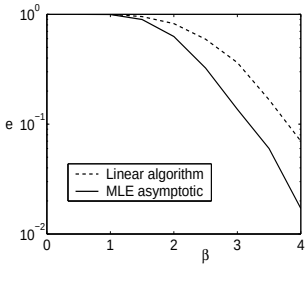

Figure 5: Performance evaluation using global confidence region.

Fig. 5 compares the performance of our linear algorithm with the MLE for the same polygon and parameters used in Fig. 4. The probabilities e_{MLE} and e_{alg} were calculated using 1000 instances of $\hat{\mathbf{s}}_{MLE}$ and $\hat{\mathbf{s}}_{alg}$ respectively. To generate $\hat{\mathbf{s}}_{MLE}$ samples, we start by drawing EGI samples from the normal distribution $N(\mathbf{\Psi}, \mathbf{C}_{\mathbf{\Psi}})$ where $\mathbf{C}_{\mathbf{\Psi}}$ corresponds to the CRLB used in (12). The $\hat{\mathbf{s}}_{MLE}$ samples can now be obtained from the EGI samples using (9). The $\hat{\mathbf{s}}_{alg}$ samples are obtained using Monte-Carlo simulations of our linear algorithm. As observed in Fig. 5, the performance of our linear estimator is close to the optimal MLE estimator.

6. Conclusions and Further Work

An efficient method for estimating a shape from its noisy EGI was proposed and using it we successfully reconstructed the confidence regions for the problem of shape reconstruction from brightness functions. However, the problem of reconstructing a 3-D shape from its noisy EGI is a very hard problem that has not yet been systematically studied. This forms a challenging direction of future research. It will be also interesting to study shape from silhouettes and shape from support functions using confidence region analysis.

References

[1] N. Ahuja and J. Veenstra. Generating octrees from object silhouettes in orthographic views. *IEEE Transactions on Pattern Analysis and Machine Intelligence*, 11(2):137–149, 1989.

[2] R. J. Gardner. *Geometric Tomography*. Cambridge University Press, 1995.

[3] R. J. Gardner and P. Milanfar. Shape reconstruction from brightness functions. In *SPIE Conference on Advanced Signal Proccessing Algorithms, Architecture, and Implementations X*, pages 234–245, 2001.

[4] R. J. Gardner and P. Milanfar. Reconstruction of convex bodies from brightness functions. *Discrete and Computational Geometry*, 29:279–303, 2003.

[5] L. Giacomini. Asteroids shapes and rotation: what is a lightcurve? `http://spaceguard.ias.rm.cnr.it/tumblingstone/issues/special-palermo/lightcurve.htm`.

[6] B. K. P. Horn. *Robot Vision*. The MIT Press and McGraw-Hill Book Company, 1986.

[7] S. Kay. *Fundamentals of Statistical Signal Processing*. Prentice-Hall, Englewood Cliffs, 1993.

[8] A. Laurentini. The visual hull concept for silhouette-based image understanding. *IEEE Transactions on Pattern Analysis and Machine Intelligence*, 16(2):150–162, 1994.

[9] A. S. Lele, S. R. Kulkarni, and A. S. Willsky. Convex polygon estimation from support line measurements and applications to target reconstruction from laser radar data. *Journal of Optical Society America*, 9:1693–1714, 1992.

[10] J. J. Little. An iterative method for reconstructing convex polyhedra from extended gaussian images. In *Proceedings AAAI National Conference on Artificial Intelligence*, pages 247–250, 1983.

[11] A. Poonawala. Shape reconstruction from support-type data. Master's thesis, Department of Computer Engineering, University of California, Santa Cruz, 2003.

[12] A. Poonawala, P. Milanfar, and R. J. Gardner. A statistical analysis of shape recontruction from areas of shadows. In *Asilomar Conference on Signal Systems and Computers*, pages 916–920, 2002.

[13] A. S. Rao and K. Y. Goldberg. Shape from diameter: Negative results. Technical Report RUU-CS-93-16, Department of Computer Science, Utrecht University, April 1993.

[14] J. C. Ye, Y. Bresler, and P. Moulin. Asymptotic global confidence regions in parametric shape estimation problems. *IEEE Transactions on Information Theory*, 46(5):1881–1895, 2000.